Terbit *online* pada laman web jurnal : http://metal.ft.unand.ac.id

**METAL: Jurnal Sistem Mekanik dan Termal**

| ISSN (Print) 2598-1137 | ISSN (Online) 2597-4483 |

Research Article

# Design and Implementation of A 50 Wp PV System for An Agricultural Grain Stirring-Collecting Robot

*Padhlani Qurrata Ayun* [ab], *Abdul Kadir Muhammad* [ab], *Arman* [a], *Ariawan Bayu Wicaksono* [ab*]

[a] *Department of Mechanical Engineering, Politeknik Negeri Ujung Pandang, Makassar, Indonesia*

[b] *Center for Mechatronics and Control System, Jurusan Teknik Mesin Politeknik Negeri Ujung Pandang, Makassar, Indonesia*

ARTICLE INFORMATION

*Article History:*
Received: 7 July 2026
Revised: 28 October 2026
Accepted: 30 October 2026

KEYWORDS

Smart Agriculture

Agricultural Technology

Agricultural Robot

Photovoltaic System

Appropriate Technology

CORRESPONDENCE

E-mail: ariawanbayu@poliupg.ac.id

**A B S T R A C T**

The use of agricultural robots in post-harvest grain drying requires a reliable and portable energy system that can support field operation without limiting robot mobility. This study aimed to design, implement, and evaluate a 50 Wp photovoltaic (PV) system as an integrated power supply for an agricultural grain-stirring and collecting robot. An applied engineering approach was used through system design, assembly, and functional testing. The developed system consisted of a 50 Wp solar panel, solar charge controller, 12 V battery, electronic control unit, and DC motor loads integrated with the robot structure. Mechanical design focused on panel placement, frame stability, and tilt-angle adjustment, while electrical testing measured panel voltage and current under outdoor conditions. Motion testing evaluated motor performance and robot movement with and without a 30 kg load. The results showed that the PV system was successfully installed without disturbing the robot's stirring, collecting, storage, and movement mechanisms. The solar panel produced average voltages of 20.16 V and 19.91 V during two-day testing, which were suitable for battery charging. The DC and power window motors operated stably at around 12.20–12.40 V, and the robot achieved speeds of 0.38–0.46 m/s. These findings indicate that a small-scale PV system can support mobile agricultural robots and promote cleaner, more energy-independent post-harvest technology.

## 1. INTRODUCTION

The development of modern agricultural technology has encouraged the implementation of smart farming as an approach to improve the efficiency, productivity, and sustainability of agricultural production processes. One application of this technology is the use of agricultural robots in post-harvest activities, including grain drying. In conventional drying processes, grain turning, stirring, and collecting are still commonly performed manually, requiring considerable labor, time, and supervision [1], [2]. This condition indicates the need for technological innovation that can assist farmers in optimizing the grain drying process, particularly through the use of robots that are able to operate more practically, systematically, and in accordance with field operational requirements [3], [4].

A grain stirring and collecting robot is a relevant solution because it can support the uniform drying process through a stirring mechanism and facilitate the collection of grain after sun drying. This type of robot operates in an open-field environment, therefore, it requires a portable, stable, and reliable energy system to support actuator performance during operation [5], [6], [7]. Energy availability is an important aspect because the robot's

https://doi.org/ 10.25077/metal.10.2.100-110.2026

This is an Open Access article distributed under the terms of the Creative Commons Attribution-NonCommercial-ShareAlike 4.0 International License

performance is not only determined by its mechanical design and control system, but also by the suitability of its power supply to the electrical load characteristics of the robot [8], [9]. Therefore, a photovoltaic (PV) system, or solar power generation system, is a potential alternative because it can provide electricity from renewable energy sources, particularly for agricultural devices operating under direct sunlight exposure [10], [11].

The urgency of this research lies in the need to design an energy system that can directly support the operation of an agricultural robot without interfering with its mechanical functions. The PV system applied to the robot should not merely be considered as an additional power source, but must be designed as an integrated system that includes mechanical aspects, electronic components, power capacity, component layout, and compatibility with the robot's operational load. In this study, the PV system was designed using a 50 Wp solar panel, a 12 V operating voltage, a Solar Charge Controller (SCC), a battery, and Direct Current (DC) loads on the robot. The testing was conducted in a 4 m × 3 m working area with a grain load of 30 kg. Therefore, the developed design is not only conceptual, but also directed toward practical implementation under the actual working conditions of an agricultural robot.

Several previous studies have discussed the development of grain-stirring robots, particularly in terms of mechanical control systems, wireless connectivity, and the integration of the Internet of Things (IoT) for remote control and monitoring of environmental parameters such as temperature and humidity. The studies conducted by Habriansyah, Saswito, and Chairany indicate that the development of grain-stirring robots has mainly focused on improving control functions, monitoring systems, and robot working mechanisms [12], [13], [14]. However, the discussion of solar-energy-based power supply systems for such robots has not yet become a major focus. Several studies only mention the use of solar energy or solar panels as the robot power source, but they do not explain in detail the PV system component configuration, panel capacity, the connection among the solar panel, solar charge controller (SCC), battery, and the integration of the system with the robot actuator load.

The research gap is also evident in studies on small- to medium-scale photovoltaic (PV) systems, which generally focus more on lighting applications, practicum modules, monitoring systems, or IoT-based load control systems [15], [16], [17]. These studies have made important contributions to the development of solar energy systems. However, they have not specifically examined the application of a 50 Wp PV system as a portable power supply installed directly on a mobile agricultural robot. This condition indicates that the integration of small-scale solar energy systems and agricultural robots still requires more applied investigation, particularly in the context of design, implementation, and basic functional testing of the PV system according to the operational requirements of robots in field conditions.

Based on this gap, the novelty of this study lies in the design and implementation of a 50 Wp PV system as an integrated portable power supply for an agricultural grain-stirring and collecting robot. This study does not merely position the solar panel as an additional component. Instead, it designs the PV system as an integrated unit consisting of two main parts, namely the mechanical PV system and the electronic PV system. The mechanical system concerns the installation of the solar panel and supporting components on the robot structure without interfering with the robot's movement and mechanical functions. The electronic system includes the integration of a 50 Wp solar panel, SCC, 12 V battery, and the robot DC load. Therefore, this study contributes to the development of renewable-energy-based agricultural robots that are more practical, portable, and suitable for grain-drying applications in open-field areas.

The objective of this study is to design and implement a 50 Wp PV system for an agricultural grain-stirring and collecting robot. Specifically, this study aims to design a mechanical PV system that can be installed on the agricultural robot, design an electronic PV system consisting of a solar panel,

SCC, battery, and robot DC load, implement the PV system on the robot without disturbing its mechanical functions, and test the basic functionality of the PV system as the robot power supply. Through this study, the developed solar energy system is expected to serve as a basis for the development of agricultural robots that are more energy-independent, environmentally friendly, and relevant to the needs of modern agricultural technology.

## 2. RESEARCH METHODS

### 2.1 Components

The components used in this study were classified based on their operating functions, namely mechanical components, electrical components, electronic and control components, and supporting software. This classification aims to explain the role of each component in developing the grain-stirring robot prototype so that the system can operate in an integrated manner, from the mechanical structure, power system, and control system to the design and programming processes.

The mechanical components used in this study consisted of the main frame, polycarbonate wheels, a 10 mm diameter stainless-steel shaft, RS-32 chain, sprocket gears, KP000 10 mm pillow bearings, angle iron, hollow steel, bolts, and nuts. The main frame served as the supporting structure for all robot components. The polycarbonate wheels functioned as the robot's mobility medium on the grain-drying area. The shaft was used to transmit rotational motion, while the RS-32 chain and sprocket gears served as the power transmission system from the motor to the drive mechanism. The KP000 10 mm pillow bearings supported the shaft to maintain stable rotation and reduce friction. Angle iron, hollow steel, bolts, and nuts were used as structural materials and mechanical fasteners for the robot assembly.

The electrical components included a solar panel, a 12 V battery, a solar charge controller, a 37GB31ZY 12 V DC motor, and a power window DC motor. The solar panel had a capacity of 50 WP, a maximum power voltage of 17.2 V, a maximum power current of 1.16 A, an open-circuit voltage of 20.64 V, a short-circuit current of 1.3 A, and dimensions of 535 × 345 × 25 mm. The solar panel functioned as an electrical energy source by converting sunlight into electricity. The generated energy was stored in the 12 V battery, with charging regulated by the solar charge controller to ensure a safe charging process. The 37GB31ZY 12 V DC motor had a no-load speed of 140 RPM, a no-load current of 350 mA, a load torque of 11.2 kg·cm, a load speed of 110 RPM, a load current of 1 A, an output power of 10 W, and a stall torque of 27 kg·cm. This motor was used as the robot wheel drive. The power window DC motor had a speed of 60 ± 15 RPM, a no-load current of less than 5 A, a load current of less than 15 A, a stall current of less than 28 A at 12 V, a torque of 30 kg·cm, a stall torque of 100 ± 15 kg·cm, and a weight of 696 g. This motor was used to operate the grain-stirring mechanism.

The electronic and control components consisted of a NodeMCU ESP8266, a BTS7960 motor driver, an LM2596 step-down module, and limit switches. The NodeMCU ESP8266 functioned as the main microcontroller that received and processed control commands. The BTS7960 motor driver featured a full H-bridge circuit, supported currents of up to 43 A, operated at a motor voltage of 5.5–27 V DC, and used an input voltage of 3.3–5 V. This component was used to control the rotation direction and operation of the DC motors. The LM2596 step-down module reduced the 12 V supply voltage to 5 V to meet the requirements of the control circuit. The limit switches were used as motion limiters for the stirring and collecting mechanism, and bucket mechanism, allowing the system to stop at predetermined positions and preventing movement beyond the designed mechanical limits.

The software used in this study consisted of Arduino IDE and Autodesk Inventor. Arduino IDE was used to write, edit, and upload the control program to the NodeMCU ESP8266. Autodesk Inventor was used to design the mechanical structure of the robot, including the frame, component mounts, shaft, wheels, and stirring system before the fabrication process was carried out.

 https://doi.org/ 10.25077/metal.10.2.100-110.2026

## 2.2 Mechanical Design

The mechanical design of the solar power system for the agricultural robot was developed by considering the compatibility of the frame dimensions, structural stability, solar panel mounting position, and the robot's range of motion during the grain stirring and collecting processes. The solar panel support frame is positioned on the upper part of the robot to enable the panel to receive optimal sunlight exposure without interfering with the drive system and other mechanical components. The design dimensions are adjusted to the main dimensions of the robot, including the top view, front view, and side view, so that the mechanical design provides a clear representation of the shape, size, and mounting position of the solar power system on the agricultural robot. The mechanical design and its dimensions are shown in Figure 1-4.

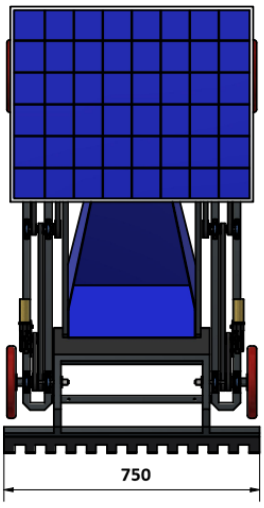



Figure 1. Top view of the agricultural robot design



Figure 2. Isometric view of the agricultural robot design

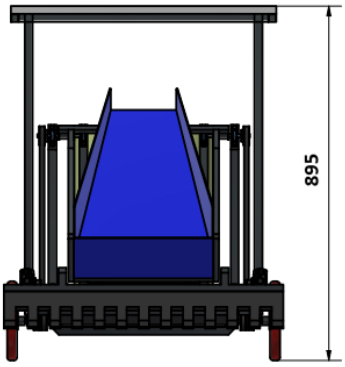



Figure 3. Front view of the agricultural robot design

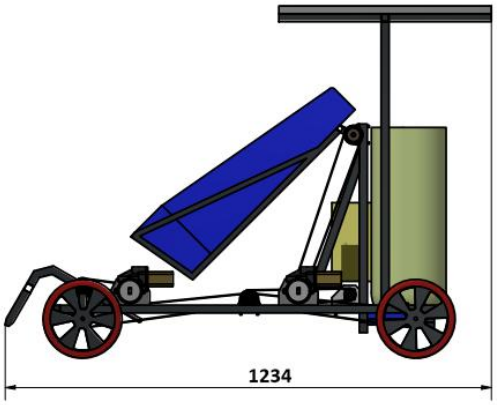



Figure 4. Side view of the agricultural robot design

## 2.3 Electrical, Electronics and Control System Design

This design consists of an electrical energy source from a solar photovoltaic system, a Solar Charge Controller (SCC), a battery, and DC loads, namely the DC motor actuator used in the robot. The electrical system design begins by calculating the total load or energy required for operation. This data analysis is conducted to determine the required capacity of the solar panel and battery to supply power to the robot load. The schematic design of the solar power generation system is then presented in Figure 5.

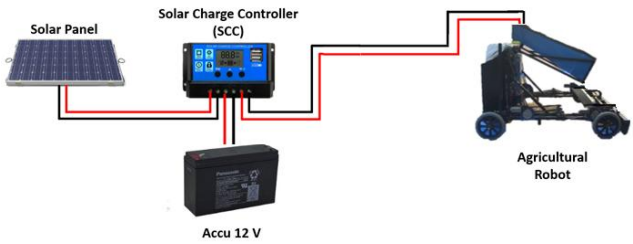



Figure 5. Electrical schematic design of the solar power generation system

In the schematic above, the solar cell functions to convert solar energy into electrical energy in the photovoltaic power generation system. The Solar Charge Controller (SCC) regulates the battery charging process and controls the battery voltage to ensure that it does not exceed the allowable tolerance limit. The electrical energy generated by the solar panel is stored in the battery and used as the energy supply for the robot. This stored energy supplies the electrical requirements of each electronic component and actuator installed on the robot. Then, Figure 6 illustrates the schematic design of the electronics and control system for the agricultural robot.

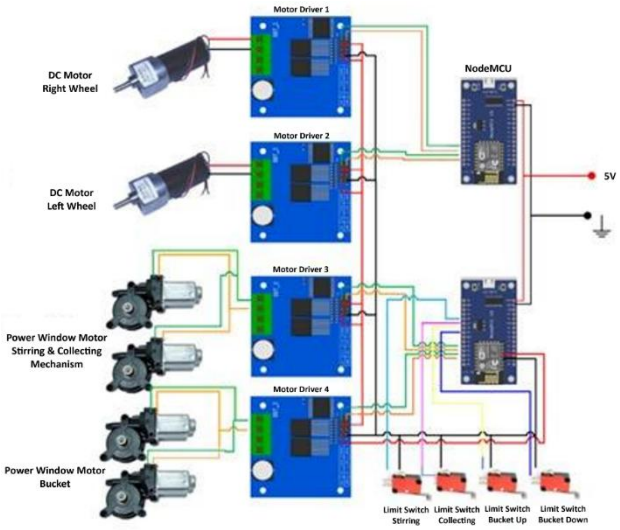



Figure 6. Electronics and control system schematic design

### 2.4 System Testing

After the robot assembly process is completed, testing will be conducted, including electrical testing and robot motion testing. Electrical testing is carried out to determine the voltage and current generated directly by the solar panel and through the solar charge controller from 11:00 a.m. to 2:00 p.m. WITA, with data recorded at 30-minute intervals. The test will be performed in an open field to ensure that the solar panel is directly exposed to sunlight. Furthermore, robot motion testing will be conducted to determine whether the DC motors, which serve as the main actuators of the robot, operate properly. This test also aims to determine the speed of the agricultural robot and to measure the voltage, current, and power consumption of the DC motors used to drive the robot. In addition, the movement speed of the agricultural robot will be measured during forward and reverse motion.

## 3. RESULTS AND DISCUSSION

### 3.1 Agricultural Robot Assembly

The mechanical system assembly results show that the agricultural robot consists of several main components, namely the main frame, solar panel, grain-stirring mechanism, grain-collecting mechanism, and grain sack storage box, as shown in Figure 7 and 8. The main frame functions as the supporting structure for all robot components, while two DC motors installed on the right and left sides of the rear section act as the main drive system, assisted by chains and sprockets to transmit motor rotation to the wheels. The grain-stirring mechanism is designed to distribute the grain evenly during the drying process, as well as to turn the grain from the upper layer to the lower layer and vice versa, so that the drying process occurs more uniformly and thoroughly. The stirrer component is made of sponge material with a length of 705 mm and a thickness of 15 mm, formed into a serrated shape with a tooth spacing of 30 mm, allowing it to stir the grain without damaging the kernels. In addition, the robot is equipped with a grain-collecting mechanism positioned directly behind the stirring mechanism and operated alternately with it. When the stirring mechanism is in operation, the collecting mechanism is lifted upward. After the drying process is completed, the collecting mechanism is lowered to direct the grain toward the center. This position-changing mechanism is driven by a DC power window motor assisted by a limit switch, which functions as a motion limiter to ensure more controlled operation. The collecting mechanism is made of sponge material with a length of 430 mm and a thickness of 10 mm to ensure that the grain collection process remains safe for the kernels. After the grain is collected in the center, the storage mechanism operates by picking up the grain using a bucket made of 0.2 mm galvanized plate.

 https://doi.org/ 10.25077/metal.10.2.100-110.2026




Figure 7. The mechanical system assembly of agricultural robot – grain stirring mechanism




Figure 8. The mechanical system assembly of agricultural robot – grain collecting mechanism

Figure 9 and 10 shows the assembled agricultural robot equipped with a solar power generation system. The solar power system is mounted on the upper part of the robot using a solar panel support mechanism designed to allow the position and tilt angle of the panel to be adjusted according to the testing requirements. The solar panel support frame is constructed from 20 × 20 mm hollow steel to provide structural strength and maintain panel stability during robot operation. The tilt angle adjustment is carried out using two M8 stainless steel bolts, allowing the solar panel to be positioned more flexibly from 0° to 45° relative to the direction of incoming sunlight. The assembly result indicates that the solar power system was successfully integrated into the agricultural robot without interfering with the main structure, drive system, or the robot's function as a grain stirring and collecting device.

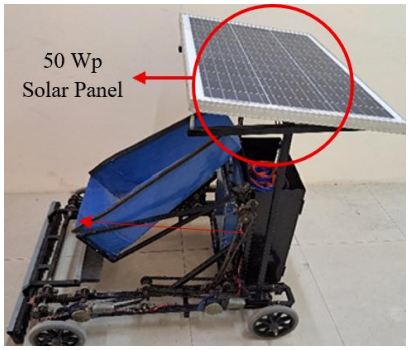



Figure 9. Agricultural Robot with a 50 Wp solar panel

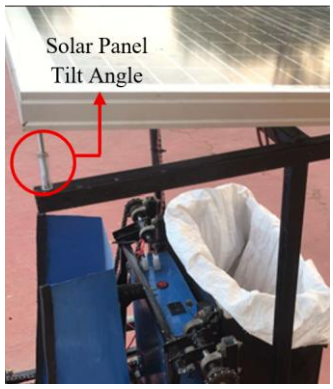



Figure 10. Solar panel tilt angle adjustment mechanism

The photovoltaic power generation system integrated into the agricultural robot is equipped with a Solar Charge Controller (SCC) and a 12 V battery as the main components for electrical energy storage and regulation. The solar panel functions to convert solar irradiance into electrical energy, which is then delivered to the SCC to regulate the battery charging process and ensure that the voltage and current remain within safe operating limits. The 12 V battery serves as an electrical energy storage unit that supplies power to the DC loads of the robot, particularly the drive motors and other supporting electrical components. The assembly results indicate that the photovoltaic system components are fully integrated, starting from the solar panel, SCC, and battery to the robot load. Therefore, the system can operate as a renewable energy-based power supply for the agricultural grain-stirring and collecting robot. Figure 11 presents the electrical configuration of the photovoltaic system installed on the agricultural robot, whereas Figure 12 shows the panel box.




Figure 11. Solar charger controller (SCC)

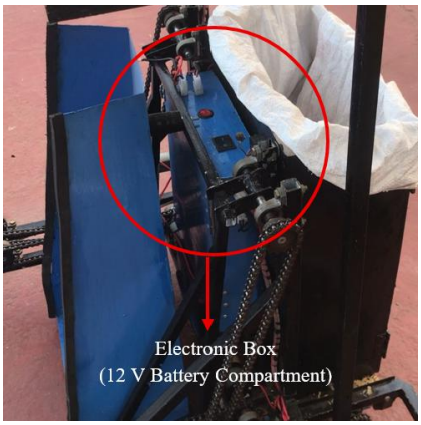


Figure 12. Electronic box

The integration results indicate that the 50 Wp PV system can be functionally implemented as a portable renewable-energy power supply for the agricultural grain-stirring and collecting robot. This finding directly responds to the research gap identified in previous studies, where grain-stirring robot development has mainly focused on mechanical control systems, wireless connectivity, and IoT-based monitoring, while the detailed configuration of solar-energy-based power supply systems has not been discussed comprehensively [12], [13], [14]. The successful installation of the solar panel, support frame, SCC, and 12 V battery demonstrates that the PV system can be integrated into the robot as a unified mechanical and electrical system without interfering with the main structure, drive system, or the robot's function in stirring and collecting grain.

This result also strengthens the novelty of the study, because the PV system is not merely used as an additional energy source, but is designed as an integrated unit consisting of a mechanical PV system and an electronic PV system, including panel mounting, tilt-angle adjustment, SCC regulation, battery storage, and connection to the robot DC load. Compared with previous small to medium scale PV studies that mainly focused on lighting applications, practicum modules, monitoring systems, or IoT-based load control [15], [16], [17], the present work shows a more applied contribution by installing a 50 Wp PV system directly on a mobile agricultural robot. Therefore, the integration result confirms that the developed PV system is feasible as an energy-supporting system for open-field agricultural robot applications, although further optimization is still required in terms of panel angle adjustment, battery capacity, and real-time power monitoring.

### 3.2 Electrical Testing Results

The testing was conducted to measure the voltage and current generated by the solar panel installed on the agricultural robot. The test was carried out by adjusting the angle of the solar panel using the solar panel angle adjustment mechanism. Data collection was conducted at the Basketball Court of Politeknik Negeri Ujung Pandang, located at coordinates 5°07′49″ S latitude and 119°2′56″ E longitude, obtained using the Google Earth application. The tilt angle of the solar module (β) was determined by first calculating the maximum solar altitude angle in degrees (α) using Equation 1 as follows.

$$A = 90° - \text{lat} + \delta \text{ (N hemisphere)} \quad (1)$$
$$A = 90° + \text{lat} - \delta \text{ (Shemisphere)} \quad (2)$$

Thus,

$$\alpha = 90° + lat - \delta$$
$$\alpha = 90° + 5.07 - 23.45$$
$$\alpha = 71.62°$$

Meanwhile, the angle that the solar panel must form relative to the Earth's surface (β) can be determined using Equation 3 as follows.

$$\beta = 90° - \alpha \quad (3)$$

Thus,

$$\beta = 90° - 71.62°$$
$$\beta = 18{,}38° \approx 18°$$

Based on these calculations, the solar panel was adjusted to form an angle of 18° to maximize the direction of incoming solar radiation. Tables 1 and 2 show the voltage and current measurement results generated by the solar panel from 11:00 to 14:00 WITA on the first and second days, respectively.

Table 1. Measurement results of solar panel voltage and current on the first day

 https://doi.org/ 10.25077/metal.10.2.100-110.2026

| Time | Weather | Solar Irradiance ($W/m^2$) | Voltage (V) | Current (A) |
|---|---|---|---|---|
| 11:00 | Sunny | 9.79 | 17.31 | 0.65 |
| 11:30 | Sunny | 1058 | 19.87 | 0.62 |
| 12:00 | Sunny | 1063 | 20.47 | 0.38 |
| 12:30 | Sunny | 1040 | 20.64 | 0.32 |
| 13:00 | Sunny | 903.50 | 21.05 | 0.21 |
| 13:30 | Sunny | 851 | 21.09 | 0.19 |
| 14:00 | Sunny | 820 | 20.70 | 0.12 |

Table 2. Measurement results of solar panel voltage and current on the second day

| Time | Weather | Solar Irradiance ($W/m^2$) | Voltage (V) | Current (A) |
|---|---|---|---|---|
| 11:00 | Sunny | 1035 | 18.19 | 0.65 |
| 11:30 | Sunny | 1041 | 19.87 | 0.62 |
| 12:00 | Sunny | 1052 | 20.27 | 0.38 |
| 12:30 | Sunny | 1023 | 20.58 | 0.32 |
| 13:00 | Sunny | 865.90 | 20.41 | 0.21 |
| 13:30 | Sunny | 815.80 | 20.03 | 0.19 |
| 14:00 | Sunny | 760 | 20.01 | 0.14 |

Based on Tables 1 and 2, the solar panel voltage during the two-day test showed relatively stable values. On the first day, the average voltage was 20.16 V, while on the second day it was 19.91 V. These values were higher than the 12 V system voltage, indicating that the panel output was suitable for supporting battery charging through the Solar Charge Controller (SCC). A photovoltaic panel converts solar radiation into electrical energy. However, its actual output under field conditions may differ from standard conditions because it is affected by irradiance and module temperature [18], [19], [20]. The standard test conditions for photovoltaic panels generally refer to an irradiance of 1000 W/m² and a module temperature of 25 °C [21], [22]. Therefore, the voltage range of 18.19 to 21.09 V indicates that the PV system installed on the robot operated within an appropriate range to support the robot electrical system.

The test results also showed that the solar panel current tended to decrease from 11:00 to 14:00 WITA. On both testing days, the highest current was recorded at 0.65 A at 11:00 WITA. It then decreased to 0.12 A on the first day and 0.14 A on the second day at 14:00 WITA. The output current of a photovoltaic panel is strongly related to the intensity of solar radiation. According to [23], when irradiance decreases, the amount of light energy received by solar cells also decreases, which results in a lower generated current. This explains why the decrease in irradiance after midday was followed by a decrease in current on both testing days.

The differences in voltage and current between the first and second days were relatively small. This indicates that the solar panel was able to produce consistent electrical output under clear weather conditions. Photovoltaic performance is mainly affected by two factors, namely irradiance and temperature. Irradiance has a stronger effect on current, while temperature can affect voltage [18], [22]. Therefore, the maximum voltage does not always occur when irradiance or current reaches its highest value. This condition was observed on the first day, when the highest voltage of 21.09 V occurred at 13:30 WITA, although the current had already decreased to 0.19 A.

Based on these test results, the 50 Wp PV system can function as an integrated renewable energy source for the grain stirring and collecting robot. The generated voltage supports energy storage in the battery, while the battery helps maintain a stable power supply for the robot electrical components and actuators. The integration of the solar panel, SCC, battery, and DC load shows that the designed energy system is suitable for the operational requirements of the robot in a grain drying area. Therefore, the application of PV technology in this agricultural robot can improve energy independence, support the use of clean energy, and strengthen the role of the robot as a practical agricultural technology for outdoor post-harvest activities.

### 3.3 Agricultural Robot Motion Testing Results

The first test was conducted to determine whether the DC motor actuator and power window motor could operate using electrical energy supplied by the solar power generation system. The test was carried out under two conditions: without load and with a working load of 30 kg. The test results for the

DC motor and power window motor, including the voltage and current supplied to each motor, are presented in Tables 3-5.

Table 3. DC motor testing data

| Load Condition | DC Motor 1 | | DC Motor 2 | |
|---|---|---|---|---|
| | Voltage (V) | Current (A) | Voltage (V) | Current (A) |
| With Load | 12.30 | 1.30 | 12.20 | 1.20 |
| Without Load | 12.40 | 1.30 | 12.35 | 1.30 |

Table 4. Power window motor 1 and 2 testing data

| Load Condition | Power Window Motor 1 | | Power Window Motor 2 | |
|---|---|---|---|---|
| | Voltage (V) | Current (A) | Voltage (V) | Current (A) |
| With Load | 12.20 | 1.20 | 12.20 | 1.20 |
| Without Load | 12.40 | 1.32 | 12.40 | 1.32 |

Table 5. Power window motor 3 and 4 testing data

| Load Condition | Power Window Motor 1 | | Power Window Motor 2 | |
|---|---|---|---|---|
| | Voltage (V) | Current (A) | Voltage (V) | Current (A) |
| With Load | 12.25 | 1.20 | 12.25 | 1.20 |
| Without Load | 12.35 | 1.32 | 12.35 | 1.32 |

Based on Table 3, the two DC drive motors of the robot were able to operate under both loaded and unloaded conditions. The motor voltage ranged from 12.20 to 12.40 V, which remains suitable for a 12 V motor system. Under the loaded condition, DC Motor 1 produced a voltage of 12.30 V and a current of 1.30 A, while DC Motor 2 produced a voltage of 12.20 V and a current of 1.20 A. Under the unloaded condition, the voltage slightly increased to 12.40 V and 12.35 V, with both motors drawing a current of 1.30 A. These results indicate that the power supply system remained stable when the robot was subjected to a 30 kg load. Theoretically, a DC motor requires current to generate torque. When the mechanical load increases, the motor must produce greater torque to maintain motion. The slight voltage drop under the loaded condition may be caused by power losses in the cables, the internal resistance of the battery, and the power demand of the transmission system. However, the relatively small change in current indicates that the load could still be handled properly by the motors and the robot drive system.

Based on Table 4 and 5, the four power window motors also showed relatively stable performance. Under the loaded condition, all motors operated at a voltage range of 12.20 to 12.25 V with a current of 1.20 A. Under the no-load condition, the voltage increased to 12.35 to 12.40 V, while the current was 1.32 A. This difference was relatively small, indicating that the stirring, collecting, and bucket mechanisms did not significantly disturb the stability of the electrical system. An electric motor equipped with a gearbox can help increase the output torque, allowing the motor to drive the mechanism even under working. The slightly higher no-load current may be affected by motor rotational speed, mechanical friction, measurement time, or the operating characteristics of the motor when it does not receive direct resistance. In conclusion, the test results show that the DC motors and power window motors can operate properly using electrical energy supplied by the PV system, both under no-load conditions and with a 30 kg working load.

The next test was conducted to evaluate the travel speed of the agricultural robot. The test was carried out by moving the robot over a distance of 28 meters under two conditions, namely without load and with a 30 kg working load. The DC motors were set to rotate at maximum speed with a PWM value of 1024. Table 6 presents the speed data of the agricultural robot during forward and reverse motion.

Table 6. Agricultural robot speed

| Load Condition | Motion | Distance (m) | Time (s) | PWM | Velocity (m/s) |
|---|---|---|---|---|---|
| With Load | Forward | 28 | 72 | 1024 | 0.38 |
| | Reverse | 28 | 70 | 1024 | 0.40 |
| Without Load | Forward | 28 | 64 | 1024 | 0.44 |
| | Reverse | 28 | 61 | 1024 | 0.46 |

Based on Table 6, the agricultural robot was able to travel a distance of 28 m at the maximum PWM value of 1024. Under a 30 kg load, the robot achieved a speed of 0.38 m/s in forward motion and

 https://doi.org/ 10.25077/metal.10.2.100-110.2026

0.40 m/s in reverse motion. Under no-load conditions, the speed increased to 0.44 m/s in forward motion and 0.46 m/s in reverse motion. These results indicate that the applied load reduced the robot speed by approximately 13.6% during forward motion and approximately 13% during reverse motion. This decrease is reasonable because the 30 kg load increases rolling resistance, mechanical friction, and the torque demand of the DC motors. When the mechanical load increases, the motor requires greater torque, so part of the supplied energy is used to overcome load resistance and transmission losses rather than solely increasing wheel rotation [36]. The slightly higher speed in reverse motion than in forward motion may be affected by load distribution, transmission direction, wheel contact with the track surface, or different mechanical losses in each direction of movement.

Compared with similar postharvest robots, such as GrainBot [3], which is designed to collect dried grain using a wheel-based system and Android control, and a cocoa bean stirring robot whose speed must be adjusted according to the stirring process requirements, the speed range of 0.38 to 0.46 m/s can be categorized as normal for a small-scale agricultural robot prototype. This speed is not excessive and remains suitable for maintaining motion stability and reducing the risk of disturbance during grain collection or stirring operations. Therefore, the testing results show that the robot drive system operates properly, remains stable, and is feasible for use in grain-drying areas under both loaded and no-load conditions.

## 4. CONCLUSSIONS

This study successfully designed and implemented a 50 Wp photovoltaic system as an integrated portable power supply for an agricultural grain-stirring and collecting robot. The results show that the mechanical PV system, electronic configuration, solar charge controller, battery, and DC loads can be integrated into the robot structure without disrupting its main movement, stirring, collecting, and storage mechanisms. Electrical testing indicates that the solar panel can provide suitable output for battery charging and support the robot's 12 V electrical system under outdoor conditions. Motion testing also confirms that the DC motors and power window motors can operate properly under both no-load and loaded conditions, while the robot maintains stable movement during forward and reverse operation. These findings demonstrate that a small-scale PV system can support the energy needs of mobile agricultural robots and contribute to the development of more practical, energy-independent, and environmentally friendly post-harvest technology. Future research should optimize panel positioning, battery capacity, power monitoring, and longer field testing under varied weather and operational conditions.

## REFERENCES

[1] C. Lytridis *et al.*, "An Overview of Cooperative Robotics in Agriculture," *Agronomy*, p., 2021, doi: 10.3390/agronomy11091818.

[2] A. Nebrida, "Smart integration in agriculture: an Arduino-driven rice grain dryer for optimal post-harvest management," *Journal of Electrical Systems and Information Technology*, vol. 11, p., 2024, doi: 10.1186/s43067-024-00170-0.

[3] S. Masiado *et al.*, "GrainBot: An Android-Controlled Rice Grain Collector Robot," *International Journal of Advanced Science Computing and Engineering*, p., 2025, doi: 10.62527/ijasce.7.2.258.

[4] J. Tuanama-Aguilar *et al.*, "Construction of an Automated Removal Robot for the Natural Drying of Cacao Beans," *Sensors (Basel)*, vol. 25, p., 2025, doi: 10.3390/s25051520.

[5] A. Chand *et al.*, "Design and Analysis of Photovoltaic Powered Battery-Operated Computer Vision-Based Multi-Purpose Smart Farming Robot," *Agronomy*, p., 2021, doi: 10.3390/agronomy11030530.

[6] A. Ghobadpour, A. Cárdenas, G. Monsalve, and H. Mousazadeh, "Optimal Design of Energy Sources for a Photovoltaic/Fuel Cell Extended-Range Agricultural Mobile Robot," *Robotics*, vol. 12, p. 13, 2023, doi: 10.3390/robotics12010013.

[7] S. Patted, K. K, K. B. D, and S. R, "Solar Powered Automated Multitasking Agricultural Robot," *IJIREEICE*, p., 2024, doi: 10.17148/ijireeice.2024.12423.

[8] [8] K. Luo, Y. Chen, R. Lin, C. Liang, and Q. Zhang, "A Portable Agriculture

Environmental Sensor with a Photovoltaic Power Supply and Dynamic Active Sleep Scheme," *Electronics (Basel).*, p., 2024, doi: 10.3390/electronics13132606.

[9] C. Xu, Y. Song, M. Han, and H. Zhang, "Portable and wearable self-powered systems based on emerging energy harvesting technology," *Microsyst. Nanoeng.*, vol. 7, p., 2021, doi: 10.1038/s41378-021-00248-z.

[10] M. A. Z. Abidin, M. Mahyuddin, and M. A. A. M. Zainuri, "Solar Photovoltaic Architecture and Agronomic Management in Agrivoltaic System: A Review," *Sustainability*, p., 2021, doi: 10.3390/su13147846.

[11] S. Ghasemi and I. Sadeghkhani, "Toward Sustainable Energy-Agriculture Synergies: A Review of Agrivoltaics Systems for Modern Farming Practices," *Solar RRL*, vol. 9, p., 2025, doi: 10.1002/solr.202500041.

[12] A. Chairany, R. Buaton, and R. Puspadini, "Penerapan Internet of Things pada Mekanik Prototipe Robot Pengaduk Gabah," *Repeater : Publikasi Teknik Informatika dan Jaringan*, p., 2025, doi: 10.62951/repeater.v3i3.617.

[13] I. Habriansyah *et al.*, "Kontrol Sistem Mekanik Prototipe Robot Pengaduk Gabah Berbasis Internet of Things," *Jurnal Teknik Mesin Sinergi*, p., 2023, doi: 10.31963/sinergi.v21i1.4222.

[14] A. Saswito, M. Musfirayanti, R. Tandioga, and I. Habriansyah, "Pengembangan Prototipe Robot Pengaduk Menggunakan Sensor Suhu dan Kelembaban untuk Memantau Tingkat Kekeringan Gabah Berbasis Internet of Things," *Jurnal Teknik Mesin Sinergi*, p., 2022, doi: 10.31963/sinergi.v20i1.3483.

[15] M. R. Putri, F. Setyawan, and S. Sumadi, "Sistem Kontrol Beban Dan Monitoring Daya Baterai Pada Panel Surya 50wp Untuk Aplikasi Penerangan Berbasis Internet Of Things," *Jurnal Informatika dan Teknik Elektro Terapan*, p., 2022, doi: 10.23960/jitet.v10i3.2640.

[16] A. Sifa, "Rancang Bangun Pembangkit Tenaga Surya (Plts) 200wp Untuk Suplai Daya Sistem Kendali Dan Monitoring Pemeliharaan Tanaman Media Air," *Orbith: Majalah Ilmiah Pengembangan Rekayasa dan Sosial*, p., 2023, doi: 10.32497/orbith.v19i2.5002.

[17] M. Syahwil and N. Kadir, "Rancang Bangun Modul Pembangkit Listrik Tenaga Surya (PLTS) Sistem Off-grid Sebagai Alat Penunjang Praktikum Di Laboratorium," *Jurnal Pengelolaan Laboratorium Pendidikan*, p., 2021, doi: 10.14710/jplp.3.1.26-35.

[18] M. K. S. Al-Ghezi, R. Ahmed, and M. Chaichan, "The Influence of Temperature and Irradiance on Performance of the photovoltaic panel in the Middle of Iraq," *International Journal of Renewable Energy Development*, p., 2022, doi: 10.14710/ijred.2022.43713.

[19] O. Bamisile, C. Acen, D. Cai, Q. Huang, and I. Staffell, "The environmental factors affecting solar photovoltaic output," *Renewable and Sustainable Energy Reviews*, p., 2025, doi: 10.1016/j.rser.2024.115073.

[20] S. Chtita, A. Derouich, E. Ghzizal, and S. Motahhir, "An improved control strategy for charging solar batteries in off-grid photovoltaic systems," *Solar Energy*, vol. 220, pp. 927–941, 2021, doi: 10.1016/j.solener.2021.04.003.

[21] A. Bala, M. B. Alao, A. O. Oyedun, O. O. Alabi, and M. Adamu, "Performance Evaluation of a Solar Photovoltaic (PV) Module at Different Solar Irradiance," *International Journal of Engineering and Applied Sciences*, p., 2024, doi: 10.24107/ijeas.1430556.

[22] E. S. Ward, N. Gad, L. Rabeh, and A. Yahia, "Effects of Solar Irradiance and Temperature on Photovoltaic Module Characteristics using a capacitive load method," *Menoufia Journal of Electronic Engineering Research*, p., 2023, doi: 10.21608/mjeer.2023.283915.

[23] S. N. M. Sabudin and N. M. Jamil, "Mathematical model for predicting the performance of photovoltaic system with delayed solar irradiance," *Kuwait Journal of Science*, p., 2024, doi: 10.1016/j.kjs.2024.100207.